by F. M. Ross

# Growth processes and phase transformations studied by *in situ* transmission electron microscopy

In situ transmission electron microscopy allows us to study growth processes and phase transitions which are important in semiconductor processing. It provides a unique view of dynamic reactions as they occur. In this paper we describe the use of in situ microscopy for the observation of reactions in silicides and the formation of semiconductor "quantum dots." The dynamic information obtained from these experiments enables us to understand reaction mechanisms and to suggest improvements to growth and processing techniques. We conclude with a discussion of the use of in situ microscopy for studying reactions such as electrodeposition which occur at liquid/solid interfaces.

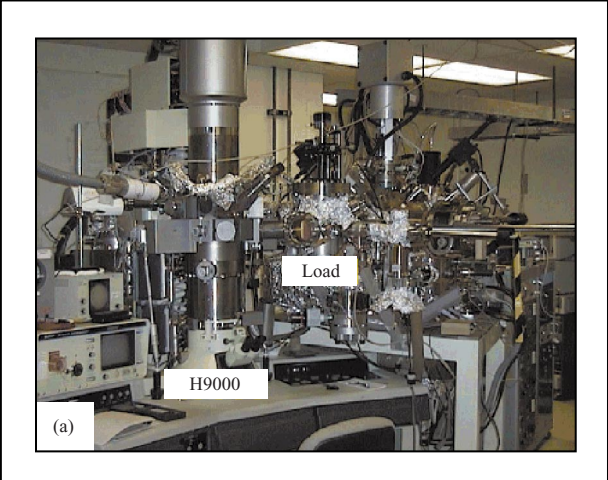
# Introduction

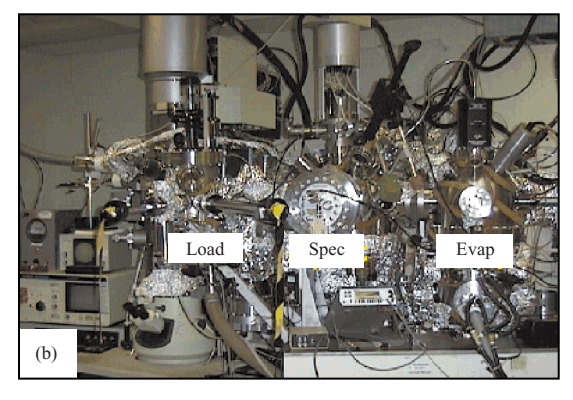
During the processing of a silicon wafer into devices, specific microstructures must be formed repeatably with a high degree of precision. Metal, insulator, and semiconductor layers of well-controlled thickness and composition must be deposited and patterned to create a composite structure with appropriate properties such as electrical resistivity or diffusion resistance. As the critical dimensions for devices become smaller, it is becoming necessary to specify precisely the crystal structures, the interface morphology, and the shapes and sizes of individual features, and control at the atomic scale is essential.

Achieving this level of control requires a detailed understanding of the fundamental processes which take place during processing. Research laboratories throughout the world have therefore been investigating reaction

©Copyright 2000 by International Business Machines Corporation. Copying in printed form for private use is permitted without payment of royalty provided that (1) each reproduction is done without alteration and (2) the Journal reference and IBM copyright notice are included on the first page. The title and abstract, but no other portions, of this paper may be copied or distributed royalty free without further permission by computer-based and other information-service systems. Permission to republish any other portion of this paper must be obtained from the Editor.

0018-8646/00/\$5.00 © 2000 IBM





The UHV transmission electron microscope: (a) View showing the microscope column and the attached loading chamber. Specimens can be transferred from the loading chamber either into the microscope or into the adjacent specimen preparation chambers. (b) View of the loading and preparation chambers. Attached to the central "spectroscopy" chamber is an electron gun for SEM and Auger analysis and an optical pyrometer for calibration of specimen temperature. The specimen can be heated by direct current while in the preparation chambers or in the microscope, and a current-temperature curve can be obtained for each specimen. In the right-hand "evaporation" chamber are two 5-kW electron-beam evaporators and an ion gun used for thinning specimens.

mechanisms and the relationship between structure and properties at all levels of integrated circuit fabrication, and as our knowledge becomes deeper, our ability to improve device performance increases. As an example of this, consider the relationship between the quality of an ultrathin gate oxide layer and the initial silicon surface on which it is grown. Studies have shown that interface steps do not move during oxidation [1]; it has therefore become clear that the initial silicon surface must be extremely

flat if a uniform oxide with a smooth interface is to be created. In the field of Al- and Cu-based chip metallization, study of the dynamics of voids has led to designs of the lines and vias which mitigate the effect of electromigration [2]. For novel devices such as single-electron transistors or solid-state lasers [3], an understanding of the growth mechanism of nanosize islands, or "quantum dots," allows these islands to be formed controllably and devices to be fabricated.

Many analytical techniques are available for studying growth and processing during the fabrication of electronic devices. In particular, transmission electron microscopy (TEM), especially in combination with advanced specimen preparation methods [4], is an indispensable technique for examining the layered structures which make up semiconductor devices. TEM has been used successfully, for example, to identify phases in polycrystalline films, to measure film texture, and in the atomic scale imaging of relevant interfaces [5]. However, most TEM investigations have relied on postprocessing examination of device structures. A full understanding of processing must also include the transient effects which occur during heating, exposure to gases, or deposition, and these effects may be timeconsuming or impossible to capture by conventional ex situ TEM analysis. We have therefore developed a transmission electron microscope in which many of the processing steps important in device fabrication can be reproduced. By observing growth and phase transitions in situ we can understand their mechanisms and model relevant processes.

In this paper we illustrate the importance of this type of in situ analysis by discussing two experiments. In the first example we describe the growth of nanosize semiconductor islands, or "quantum dots," by selfassembly during strained-layer epitaxy, and show how in situ growth of islands in the TEM allows us to observe the phenomenon of self-assembly in real time. By observing the evolution of island sizes and shapes, we were able to determine how to optimize processing conditions to achieve the narrow size distribution required for quantum dot devices. Furthermore, observations of island nucleation suggested ways to pattern the islands in particular regions of the specimen. Together these results indicated that self-assembly is a viable technique for forming quantum dots for novel devices. In the second example, we describe studies of a phase transition in the Ti-Si system. The transition from the C49 phase of TiSi<sub>2</sub>, which has a high resistivity, to the C54 phase, having a much lower resistivity, must occur consistently during processing of low-resistance contacts. Real-time observations of silicide phase formation in Ti films deposited in situ and ex situ allowed us to measure the

<sup>1</sup> See the other papers in this issue.

growth kinetics of the desirable C54 phase and to show that the propagation of the phase boundary is rate-limited by oxygen and other impurities at grain boundaries in the precursor C49 phase. These results suggested changes in processing conditions which might encourage the phase transition and thereby improve contact properties. We conclude with a discussion of a different class of growth process—electrochemical deposition of materials from a liquid solution—and show how *in situ* TEM may allow the dynamics of liquid/solid interfaces to be studied.

# Design of a transmission electron microscope for the study of growth processes

Our experiments were performed in a 300-kV Hitachi H9000 ultrahigh-vacuum transmission electron microscope (UHV TEM) having a base pressure of  $2 \times 10^{-10}$  Torr [6]. The microscope was modified to enable several types of growth process to be carried out during observation of the specimen (Figure 1). Gases are introduced to the specimen area through capillary tubes, allowing oxidation or growth by chemical vapor deposition (CVD). A pressure of up to  $10^{-5}$  Torr can be sustained with the beam on. An electron-beam evaporator mounted directly above the polepiece allows us to carry out evaporation in situ [7]. For further analysis and preparation, an Auger spectroscopy system, an ion gun, and two additional 5-kW evaporators are located in adjacent chambers to which the specimen can be transferred without breaking vacuum. Specimen heating is carried out by direct current using a double-tilt heating holder designed especially for the system.

Silicon substrate specimens were used in the present study. The specimens consisted of  $2 \times 4$ -mm rectangles cleaved from 100- $\mu$ m-thick Si(001) or Si(111) wafers which had been polished on both surfaces. They were thinned to electron transparency with an HF/HNO<sub>3</sub>/CH<sub>3</sub>COOH mixture. Final thinning was carried out by etching in the microscope polepiece using a low pressure of oxygen ( $10^{-6}$  Torr) at about  $900^{\circ}$ C until a desired thickness was achieved [1]. The specimens were then flash-heated to above  $1250^{\circ}$ C to form a clean surface on which growth could take place. Dynamic processes were recorded in real time using an image intensifier linked to a video system, or on photographic plates which were subsequently digitized for computer analysis.

# The growth and patterning of quantum dots of Ge on Si

Considerable interest has recently centered around the properties of quantum dots and their potential use in novel microelectronic devices. The term *quantum dot* refers to a volume of material which is small enough, of the order of a few nanometers or less in diameter, that

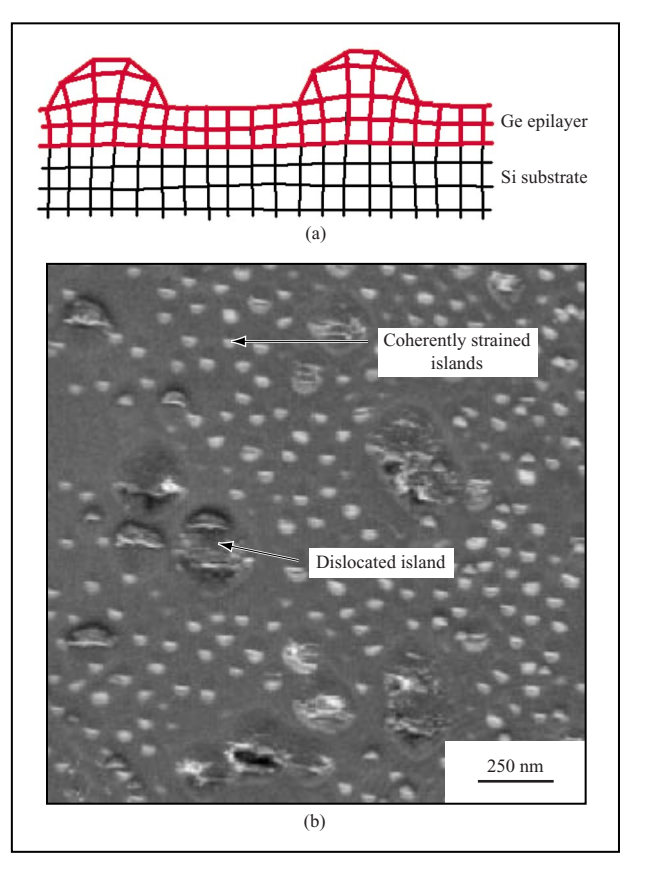


# Figure 2

(a) Schematic diagram showing epitaxial growth of Ge on Si(001). Islands form because strain can be relieved by allowing the Ge lattice to expand at the tops of the islands. (b) Ge islands formed after deposition of approximately 10 ML of Ge on Si(001). In this example the islands were not of uniform size. The small islands were coherently strained, as shown in (a), while in the largest islands a second mode of strain relief was visible: the introduction of misfit dislocations at the Ge/Si interface.

quantum confinement effects lead to unusual electronic properties. Several exciting applications for such dots have been envisaged, including single-electron transistors and lasers. For these devices to function efficiently, a well-organized group of identically sized dots is necessary. However, because of their small size, the fabrication of such dots is at present beyond the limits of conventional lithography, and an alternative technique for growth is necessary.

One very promising route to the fabrication of nanosize volumes of material is to make use of the phenomenon of island self-assembly during strained-layer epitaxial growth [8]. To illustrate how this occurs, consider the case of Ge growing epitaxially on Si (Figure 2). The Ge lattice spacing is about 4% larger than that of Si, so significant

 $<sup>\</sup>overline{^2}$  Model 622 Image Intensifier, Gatan, Inc., 680 Commonwealth Drive, Warrendale, PA 15086.

strain energy is stored in the Ge lattice as it grows. As Ge is deposited beyond about three monolayers (ML), the growing surface becomes nonplanar and islands form, relieving strain by allowing the Ge lattice to expand at the island peaks. Depending on the growth conditions, the islands may be up to 100 nm in diameter and can have a very uniform size distribution.

The spontaneous formation of nanosized islands during strained-layer growth, if it can be sufficiently well controlled, provides a means to fabricate quantum dots which bypasses the limitations of lithography. However, the self-assembly process has its own limitations: In particular, the placement of individual islands is not defined at the start of growth, and island sizes may show large variations. Thus, the critical questions in using selfassembly for quantum dot fabrication are as follows: Can we control the size (and shape) of the islands formed, and can they be grown in specific locations? Extensive study of island self-assembly in Ge/Si, as well as in other systems (InP/GaInP, InGaAs/GaAs, and CdSe/ZnSe) in which the phenomenon occurs [9], have led to some highly successful recipes for growing quantum dots with desirable properties. However, the increasing importance of these structures makes it essential to control the size distribution and placement more precisely, and this has stimulated further detailed studies.

Postgrowth examination of island populations has revealed several intriguing aspects of the self-assembly process. One particularly important result is that in many cases islands can be grown with a very narrow size distribution [10]. Although this is very convenient for device applications, the reason for the narrowness of the distribution is not well understood. The distribution is generally considered too narrow to be due to Ostwald ripening [11], and several other growth mechanisms have been proposed. Some models are based on thermodynamic arguments, postulating the existence of a minimum energy size to which islands will tend to grow [12]. Other models suggest that kinetic effects slow down the growth of larger islands, allowing the smaller ones to catch up. Possible reasons for this may be the slowing of diffusion to an island due to the strain field around it [13] or the reduced probability of nucleating a step on the surface of a larger island, again due to strain [14].

A second interesting result, so far observed only in the Ge/Si(001) system, is the recent observation of a *bimodal* island size distribution, with the two peaks corresponding to two different island shapes [15]. Smaller islands (less than about 60 nm in diameter) have been found to be square-based *pyramids*, while larger ones adopted steeper "dome" shapes with additional facets. The origin, evolution, and distribution of the pyramids and domes are

important for the development of quantum dot devices and are the subject of much debate at present.

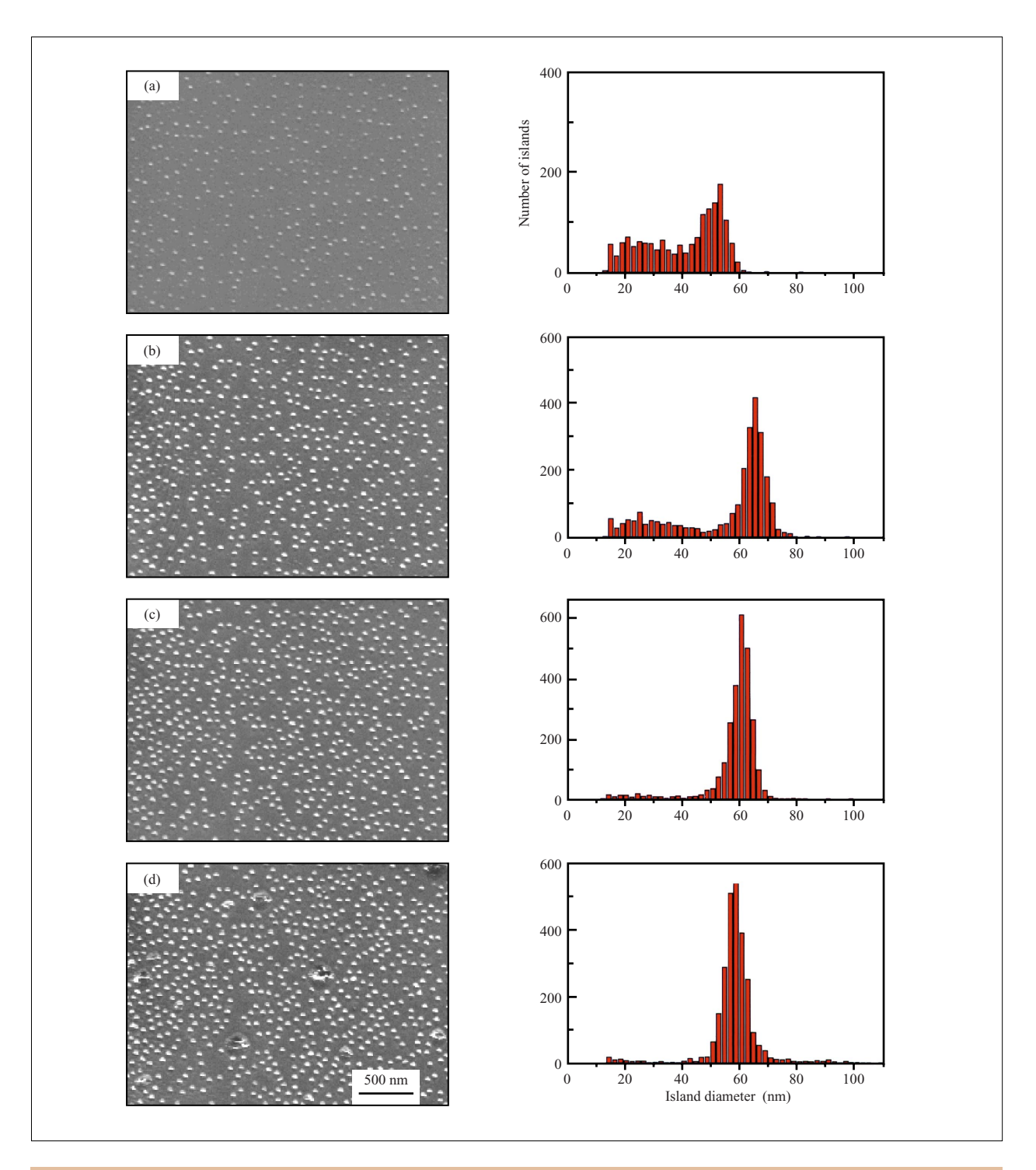
We therefore examined the process of island self-assembly in Ge on Si in real time using the *in situ* TEM system. Ge was grown by CVD on Si(001) at a specimen temperature of 650°C using digermane gas (Ge $_2$ H $_6$ ) at a pressure between 10 $^{-8}$  and 10 $^{-6}$  Torr, resulting in a growth rate of 0.1–10 monolayers of Ge per minute. A weak-beam imaging condition was chosen which showed the strain field around the islands. This allowed island positions and sizes to be resolved, although the images did not show the shapes of individual islands.

Representative results from the experiments are shown in Figures 3 and 4. The *in situ* observations revealed a rich evolutionary process. **Figure 3** indicates how the bimodal size distribution develops in a large population of islands. Shortly after islands become visible, a broad bimodal distribution develops, with two peaks corresponding (presumably) to the pyramid- and dome-shaped islands. At later times, the smaller (pyramid) peak weakens and almost disappears. While a single postgrowth observation made, for example, after 50 seconds [as in Figure 3(b)] might suggest two stable populations, the complete series shows that the pyramids are transient, with no particular size preferred, and vanish at later times. Note that the domes show their narrowest size distribution just as the pyramids are disappearing [Figure 3(c)].

To explain these results, we have developed a simple model [16] based on the existence of the two known island shapes. During growth, islands can exchange Ge atoms, since at the relatively high growth temperature of 650°C the equilibrium concentration of Ge adatoms on the surface is large ( $\sim$ 10% [17]), and Ge atoms can easily detach from an island, diffuse along the surface between the islands, and reattach to another island. Calculations show that this process occurs so readily that the flux of detaching and attaching Ge adatoms is more important in controlling the development of an island than the flux of Ge arriving from the gas phase. If one island, because of its shape or size, has a lower energy per atom than another island, Ge atoms will preferentially detach from higher-energy islands and attach to the lower-energy island. Islands can thus shrink or grow depending on their energy per atom in comparison to the other islands.

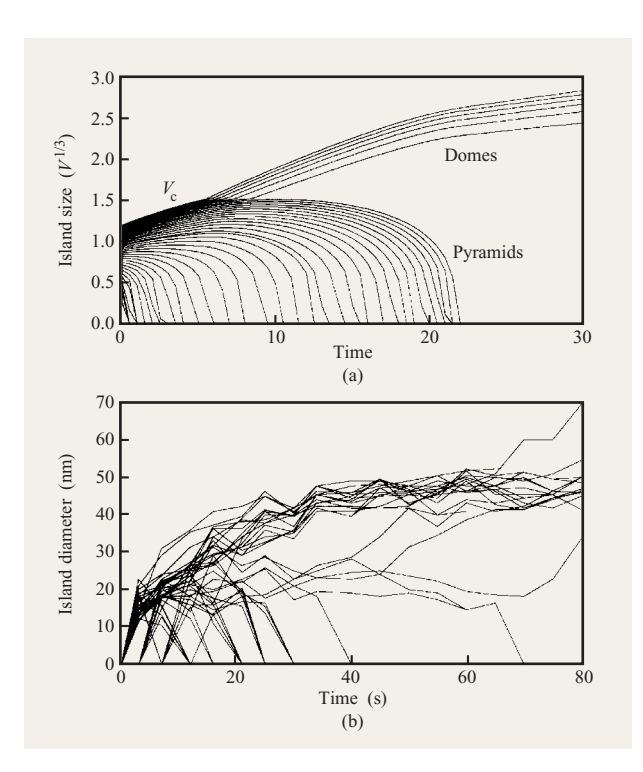
If all of the islands were the same shape, we would expect that the larger islands would always have a lower energy per atom than the smaller ones by virtue of their lower surface energy/volume ratio. The larger islands would grow at the expense of the smaller ones, leading to the well-known classical phenomenon of Ostwald ripening [11]. However, if two different island shapes are allowable,

492



Weak-beam (220) dark-field images and corresponding histograms obtained during Ge deposition from  $2 \times 10^{-7}$  Torr Ge $_2H_6$  at a substrate temperature of 640°C. The images show the same area and were taken (a) 21 s, (b) 51 s, (c) 98 s, and (d) 180 s after "nucleation" (defined as the time at which island strain contrast is first seen). Nucleation occurred after a dose of ~50 L digermane. Note that the two island shapes (pyramids and domes) cannot be distinguished in these images. The histograms were obtained by digitizing the images and using a particle-counting algorithm on the ~2600 islands visible. The distribution appears to cut off at ~15 nm diameter because the smallest islands were not detected by the algorithm owing to weak contrast. In (d) some large islands with multiple dislocations formed, creating a long tail (not shown) in the size distribution.





### Fiaure 4

(a) Simulation showing the fate of a group of islands with different initial sizes. We have assumed that islands make the transition from pyramids to domes at a critical volume  $V_c$ . The rapid growth rate of the first islands to exceed  $V_c$  leads to the subsequent bimodal size distribution. At later times, note the narrowness of the size distribution for the domes compared with the initial distribution. The scale of the plot is chosen to match the data shown below. (b) Experimental data showing the growth of all islands in a 0.5- $\mu$ m  $\times 0.5$ - $\mu$ m area. Data were measured from a video obtained during growth at  $5 \times 10^{-7}$  Torr Ge<sub>2</sub>H<sub>6</sub> and 650°C. (The islands whose trajectories terminate drifted out of the field of view during the experiment.)

the process becomes much more complex and interesting. For the Ge pyramid and dome shapes described above, simple calculations of the energy per atom show that the pyramid shape is preferred for smaller islands below a critical volume  $V_{c}$ , while the dome shape is favored at volumes greater than  $V_s$ . The islands formed during the early stages of Ge deposition are all small and therefore pyramid-shaped and undergo Ostwald ripening, with the larger islands growing at the expense of smaller ones. As the successful pyramids grow, the first few to reach the volume  $V_a$  make the transition to the dome shape. Their energy per atom rapidly decreases, making them very attractive sites for adatoms and increasing their growth rate still further at the expense of the smaller islands. The result of this process is shown in Figure 4(a), while in Figure 4(b) this model is compared with experimental

data. The model reproduces the correct trends here as well as for larger ensembles of islands such as in Figure 3, where it predicts that a population of unstable small islands will disappear to leave a relatively narrow distribution of larger islands.

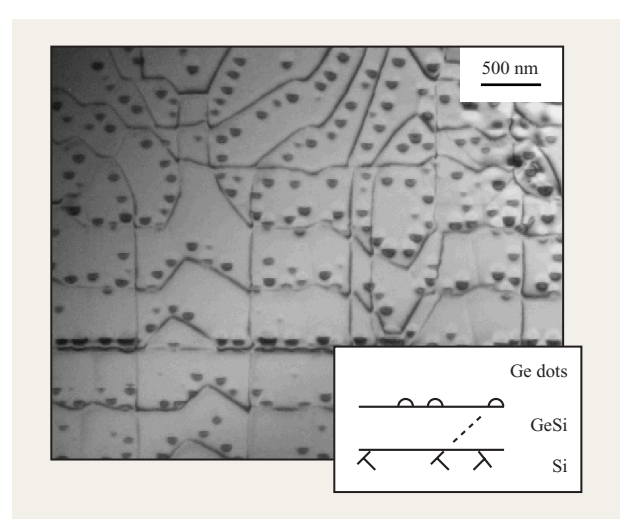
In this simple model, islands have no preferred size, but instead grow or shrink at a rate determined by their environment. Islands continue to grow as long as smaller islands are available to supply adatoms, until the final configuration, one very large island, is reached. In contrast to the models described previously [12–14], there is no factor which tends to equalize island sizes; the narrow size distribution is the result of selection of the largest islands at the volume  $V_{\rm c}$ . It is clear that for best uniformity, growth should be stopped just after the last pyramids have disappeared; further growth or annealing does not improve the island distribution.

Narrowing the island size distribution, even below the width shown in Figure 3(c), would be advantageous to the performance of real devices. One prediction from our model is that the distribution at later times can be improved only by controlling the initial nucleation of the islands. If all of the islands were to nucleate at the same time and be equally spaced, they should develop similarly and have a very narrow distribution. We have therefore looked into the factors which control island nucleation.

Any irregularity on the initial Si surface which changes the local sticking probability of Ge adatoms can influence island nucleation, and islands are known to nucleate preferentially on mesa edges [18], near clusters of dislocations [19], and near step edges [20]. However, we have found that the strain fields from individual buried dislocations provide the most convenient way of controlling island nucleation. This effect is shown in Figure 5, where a SiGe alloy was used to generate buried dislocations. Growth of the alloy above the critical thickness for dislocation formation [21] resulted in the creation of a network of misfit dislocations at the SiGe/Si interface (see inset in Figure 5). Further growth of pure Ge resulted in island growth in rows associated with the dislocations. Figure 5 shows that islands do not form directly above the dislocations but are offset to one side or the other.

The nucleation of these islands is influenced by the strain field of the dislocations, which extends up to the specimen surface. A calculation of the surface strain field due to a single dislocation<sup>3</sup> showed that the region of maximum tensile strain, where we might expect Ge atoms to stick preferentially, is offset to one side of the dislocation; the islands formed in a row at the expected location (**Figure 6**). (The nucleation of islands at this

<sup>&</sup>lt;sup>3</sup> F. M. Ross, K. Schwarz, and R. M. Tromp, work in preparation, 1999.



Ge islands formed on a 300-nm  $\mathrm{Si}_{0.8}\mathrm{Ge}_{0.2}$  alloy layer on a Si substrate. The alloy layer has partially relaxed, forming misfit dislocations at the SiGe/Si interface, and the Ge islands have grown in rows associated with these dislocations.

location was not simply an effect of the additional surface step due to the dislocation. This is because the step density was very high, typically one step every 10 nm on the surface; therefore, one extra step was not significant.)

These experiments have therefore shown that it is possible to pattern single rows of islands along individual dislocations. A two-dimensional array of dislocations should allow islands to adopt a regular pattern, resulting in a structure which may perhaps be conducive to information storage. Techniques for patterning arrays of dislocations have already been developed [22], and the fabrication of devices requiring regular arrays of quantum dots should therefore be feasible.

In summary, real-time observations of island selfassembly in Ge on Si(001) have led to the development of a simple model which can explain the dynamic changes in island population observed during growth. The presence of two island shapes leads to surprisingly complex kinetics, and since the island evolution occurs over such short time scales, it would be difficult to understand the growth process without carrying out in situ observations. From these results, we can suggest ways to approach the important problems of size control and patterning of quantum dots. In terms of size control, growth of a uniform group of islands is possible owing to the selection effect at the volume  $V_c$  and is best achieved by stopping growth just after the smaller islands have disappeared. For patterning, the strain fields of individual dislocations can influence island nucleation strongly enough to enable us to

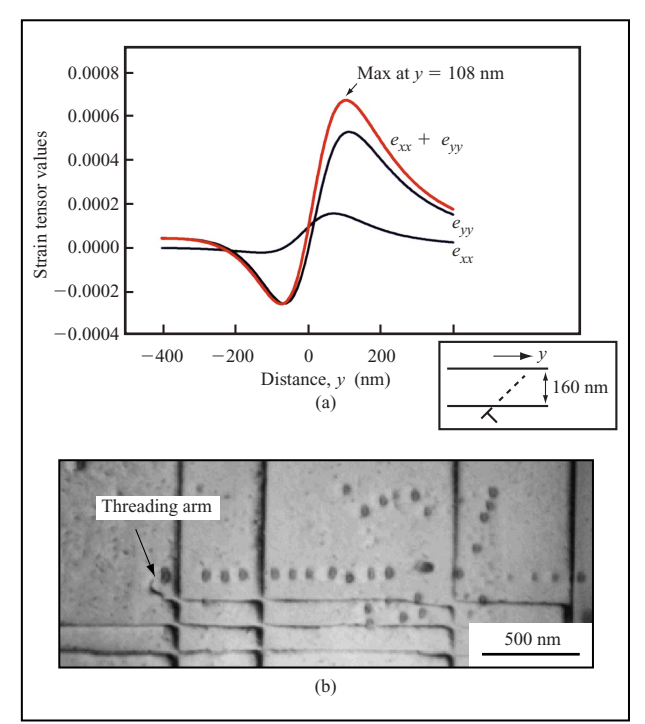


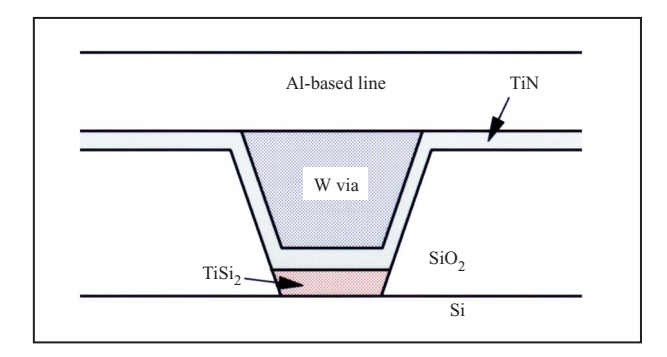
# Figure 6

(a) Calculation of the strain field at the surface associated with a single  $60^{\circ}$  misfit dislocation which is parallel to and 160 nm below the surface of a Si crystal. The maximum tensile strain  $(e_{xx} + e_{yy})$  occurs approximately at the point where the slip plane intersects the surface. (b) Ge islands grown on a 160-nm  $Si_{0.85}Ge_{0.15}$  alloy layer on a Si substrate. A single row of islands formed at the location expected from the calculation. The end of the threading arm shows where the slip plane for this particular dislocation intersected the surface.

place islands in particular areas of the surface. Taken together, these results show that islands formed by strained-layer epitaxy may play a significant role in the development of quantum dot devices.

# Phase transitions in TiSi,

TiSi $_2$  is an important component in high-density integrated circuits such as those found in random-access memory. Its use in low-resistance contacts is shown schematically in **Figure 7**. The purpose of the structure shown is to form an electrical contact between the Al-based line and the Si substrate, and this is achieved by patterning a vertical-walled via into the dielectric layer and filling it with tungsten. A thin TiN diffusion barrier is added to prevent the tungsten from diffusing into the silicon. However, electrical contact between the TiN and Si is poor, so a low-resistivity TiSi $_2$  layer is also added. This layer is formed by depositing a blanket film of  $\sim 30$  nm Ti onto areas patterned with polysilicon and SiO $_2$  and



Schematic diagram showing the  ${\rm TiSi}_2$  contact layer used in a typical via.

then annealing to form  $\mathrm{TiSi}_2$  in the polysilicon areas. The annealing, carried out at  $600-700^{\circ}\mathrm{C}$ , actually forms a high-resistivity metastable phase of  $\mathrm{TiSi}_2$  known as C49; the final step is conversion of the C49 phase to the stable C54 phase, which has a lower resistivity, by a rapid anneal at  $850-900^{\circ}\mathrm{C}$ .

The contact scheme described above is complex but works well for circuit designs with contact areas greater than about 1  $\mu$ m<sup>2</sup>. However, the miniaturization of components in integrated circuit design has reduced the area available for such contacts and led to an unexpected problem: In very small areas, the conversion of C49 TiSi<sub>2</sub> to C54 TiSi<sub>2</sub> is retarded, occurring only at temperatures above ~900°C [23]. The phase transition occurs unreliably during the 850–900°C anneal, leading to contacts with widely varying resistivities. This problem has slowed progress in the development of future generations of circuits with TiSi<sub>2</sub> contact layers, and it is therefore very important to understand why the phase transition is inhibited in small areas, and how it can be encouraged to occur at lower temperatures.

As might be expected for such an important problem, several analytical techniques have been applied to the study of the C49–C54 phase transition [24], and X-ray diffraction and ex situ microscopy studies have revealed some important features of this phenomenon. Grain sizes in the C49 and C54 phases differ by about an order of magnitude, with C49 grains around 100 nm in diameter transforming to C54 grains more than 1  $\mu$ m across. The very large size of C54 grains suggests that the nucleation of the C54 phase is difficult, and the nucleation sites for C54 have not yet been unambiguously identified. Further studies have shown that alloying Ti with other metals, such as Mo or Nb, before permitting it to react with Si can reduce the C54 grain size and improve the uniformity of the reaction in small regions. Synchrotron

X-ray experiments following the progress of the phase transition in blanket and patterned films have revealed subtle changes in reaction temperatures and film texture which reflect the underlying mechanism of the effect of these alloying elements [25].

However, one important factor which has not been addressed in these studies is the effect of impurities other than alloying metals in the films. Because Ti is such an efficient gettering agent, sputtered films of Ti contain substantial amounts of oxygen, and even relatively clean films oxidize further between growth and annealing. This effect is particularly important for the thinnest films of most interest in integrated circuit manufacturing. We have therefore used the in situ cleaning and evaporation capabilities of the UHV-TEM to examine the effect of oxygen impurities on the TiSi, phase transition. We have compared the transition in clean, UHV-deposited Ti with the transition in sputtered films which contained appreciable amounts of oxygen. The differences in reaction kinetics were striking and showed that the presence of oxygen at grain boundaries in the C49 phase causes a significant reduction in the rate of the C49-C54 phase transition.

To observe the transition *in situ*, a clean (001) Si surface was formed by repeated flashing of a thinned Si specimen to  $1300^{\circ}$ C, and a 10-nm-thick Ti film was deposited at room temperature at a pressure of less than  $5 \times 10^{-9}$  Torr. The specimen was then heated progressively in the microscope to  $850^{\circ}$ C. The phases formed were identified from images and diffraction patterns, and the reaction kinetics were recorded at video rate. A similar heating sequence was applied to a 10-nm-thick Ti film on Si(001) which had been deposited by sputtering *ex situ*; the specimen was then thinned to electron transparency by etching from the back surface.

**Figure 8** shows the phases formed during the heating of the UHV-deposited Ti film. As-deposited, the Ti film had a grain size of around 10 nm [Figure 8(a)], and annealing at low temperatures resulted in the formation of a small-grained TiSi phase (not shown). The C49 TiSi<sub>2</sub> phase appeared after heating to 700°C, while the C54 phase appeared at 850°C.

The phases formed during heating of the *ex-situ*-sputtered film appear indistinguishable from those for the UHV-deposited film, with similar grain sizes and diffraction patterns. However, the kinetics of the C49–C54 phase transformation were quite different. In **Figure 9** it can be seen that the transition occurred smoothly in the UHV-deposited film, with a large C54 grain steadily consuming the smaller C49 grains. The interface velocity was independent of the orientation of the C49 grains. In contrast, the sputtered film underwent a very jerky transformation, pinning at grain boundaries in the C49 structure, then moving rapidly across C49 grains. We attribute the differences in reaction kinetics to oxygen

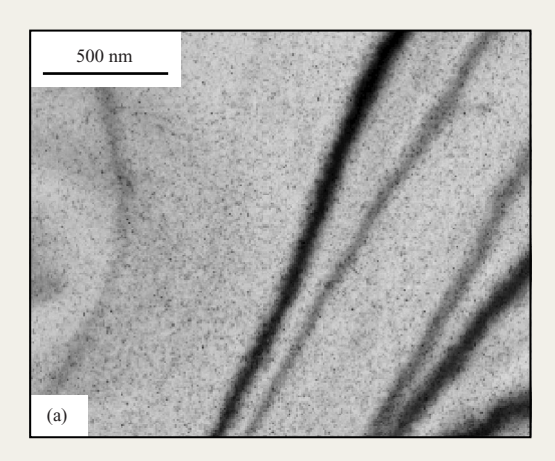
segregation at the grain boundaries. Since C49 and C54 have the same stoichiometry, the reaction in the UHV-deposited film could occur relatively easily without any need for long-range diffusion. However, the reduction in the number of grain boundaries which also occurred during the transformation requires diffusion of any grain-boundary segregants to other sites on the surface or interface. It is this process which appeared to reduce the reaction rate in the *ex-situ*-sputtered film.

This result is significant in our attempts to enhance the C49–C54 reaction rate during integrated circuit processing. For a rapid transformation, low oxygen concentrations are preferable. However, it is also advantageous to increase the nucleation density of the C54 phase so that individual reaction fronts have less distance to cover before the reaction is completed. Since the C54 nucleation density can be increased by alloying, we are now conducting further experiments to determine how oxygen impurities affect the transformation kinetics in alloyed films.

# Studying the liquid/solid interface by in situ microscopy

The preceding examples have shown how processingrelated reaction mechanisms can be observed and growth phenomena understood through in situ experiments. Many phenomena of interest during processing take place at gas/solid or solid/solid interfaces and are therefore amenable to study in situ in the TEM. However, there is an important class of growth processes which occur at a liquid/solid interface, and these have not received corresponding microscopic study. One example of topical interest is the deposition of copper by electroplating. The success of copper as a replacement for aluminum in metal lines has encouraged the study of several different copperdeposition techniques. Electroplating is the method of choice for integrated circuit fabrication, but important issues remain in applying this technique. Examples include the problem of reliably depositing copper into small vias, and the control of the microstructure of the lines (grain size and texture) to ensure good coverage and reduce electromigration.

Several phenomena are unique to the electroplating process used in integrated circuit fabrication. These include the effect of the underlying "seed layer" on grain nucleation and orientation, and a "transient grain growth" process in which grain size increases, even at room temperature, in the minutes or hours after deposition. Observations made in real time during and immediately after deposition would be helpful in understanding these phenomena. We are therefore developing a liquid cell in which electroplating, or other liquid processes, can be reproduced while under TEM observation.



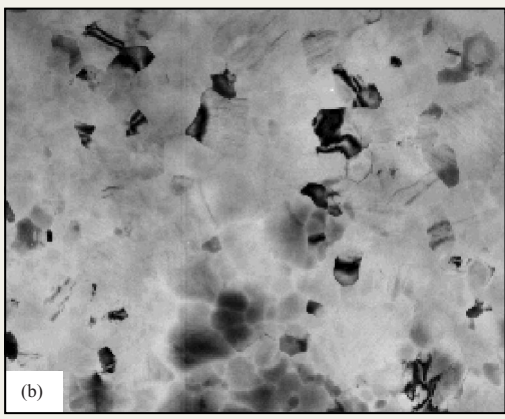
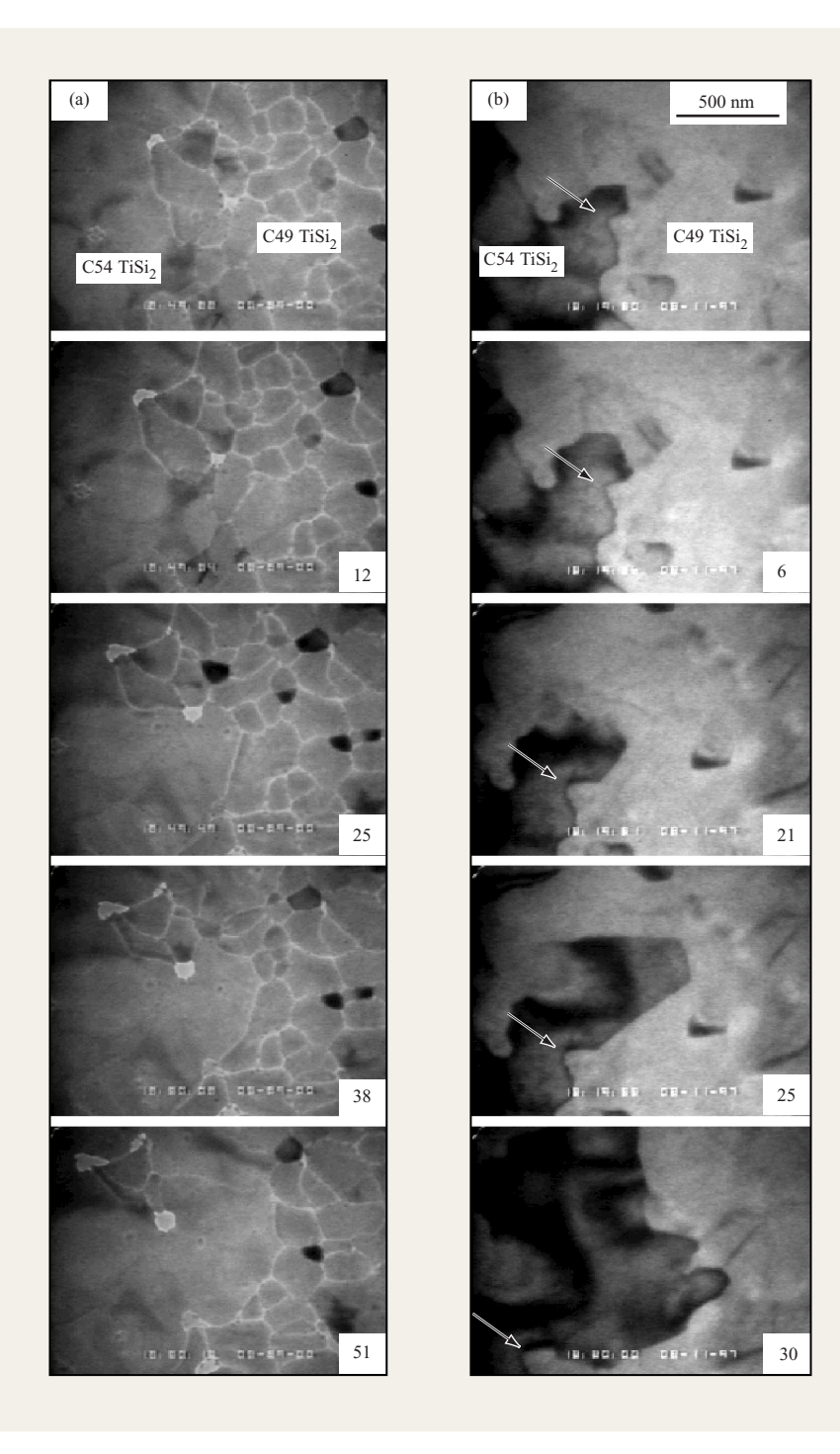




### Figure 8

Some of the phases formed during heating of a 10-nm-thick Ti film deposited under UHV on Si(001): (a) The Ti film as-deposited was microcrystalline. Heating to 300°C caused development of a fine-grained TiSi phase as well as other phases of intermediate stoichiometry (not shown). (b) After heating to 700°C, the C49 phase was identified by its faulted structure and 100-nm grain size. (c) Above 850°C, micron-sized grains of C54 were visible. The dark lines were stacking faults, and the appearance of pinholes in the film showed that it was starting to agglomerate.



Video frames showing the transformation from the C49 to the C54 phase. The numbers indicate the time elapsed in seconds since the first frame. (a) The phase transition in a 10-nm-thick UHV-deposited Ti film, recorded during heating at 825°C. The reaction front moves from left to right smoothly with no pinning. The bright feature is a pinhole. (b) Phase transition in a 10-nm film sputtered *ex situ* and containing about 33% oxygen, as measured by Auger electron spectroscopy. A single C54 grain is in a strong diffracting condition and appears dark. The C49 phase has a grain structure similar to that shown in (a), although the grain boundaries are less visible due to a greater substrate thickness. The arrow marks a reference point on the specimen. The reaction occurs in a jerky fashion with pinning events at the grain boundaries (first three frames) followed by rapid jumps across several grains (fourth and fifth frames).

The cell, shown schematically in **Figure 10**, is designed to fit into a single-tilt holder which is of standard design except for the addition of electrical connections. It is made up of two silicon-nitride-covered Si wafers which have been etched to form small windows. The wafers are glued together face to face so that these "imaging windows" are aligned, while a spacer layer keeps the windows a fixed distance apart. Two larger windows are also etched into the upper wafer, and the nitride is removed from these windows. The two etched volumes act as reservoirs for the liquid, so that a drop of liquid can be placed in one reservoir and can flow by capillary action across the imaging window. After liquid is introduced, the reservoirs are sealed by gluing sapphire squares on top of the cell.

To study electroplating, electrical contacts are patterned on the wafers before the cell is assembled (Figure 10), and a copper sulphate/sulphuric acid solution is used as the electrolyte. It is intended that plating will take place onto an anode which is visible through the imaging window. Calculations suggest that application of a potential of around 2 V will allow a current density of 10<sup>-6</sup> A/mm² to flow, depositing 200 nm of Cu in several minutes. Reversing the polarity allows the copper to be dissolved off the anode so that the experiment can be repeated. It is important to note that the volumes of copper which are to be plated are sufficiently small that the finite amount of electrolyte present is not significant.

Although the full system is still undergoing testing, we have already shown that cells of this design can hold liquids in the vacuum environment of the microscope. However, due to curvature of the SiN, the total specimen thickness (liquid, metal, and SiN) is much greater than desirable for imaging. To improve the image quality, we have recently added an energy filter to the microscope. This improves the image contrast significantly by removing electrons which have undergone inelastic scattering, allowing only elastically scattered electrons to contribute to the image. The development of the liquid cell should enable us to study many phenomena other than electrodeposition, including switching in liquid crystals and crystal growth from a solution.

## **Conclusions**

In this paper we have described the use of *in situ* TEM to analyze several phenomena which are of importance in the development of advanced integrated circuits. With its combination of high spatial resolution and video-rate image acquisition, as well as the many modes available for obtaining images (bright field, dark field, selected area diffraction, etc.), *in situ* transmission electron microscopy is a versatile means

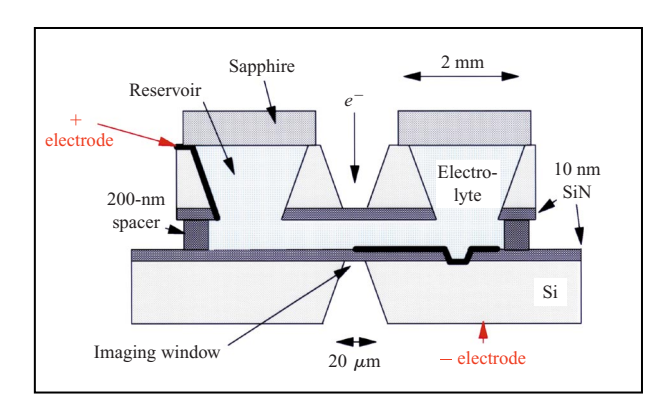


# Figure 10

Schematic diagram of experimental liquid cell. The spacer layer is formed from SiO<sub>2</sub>, and the positive electrode is formed from deposited copper. The contact to the negative electrode is achieved through a hole etched in the SiN.

for studying a wide range of phenomena in solid-state materials science, even though this is achieved at the cost of considerable experimental complexity. The development of the liquid cell should extend its applicability to the study of dynamic reactions at the liquid/solid interface. With the ever-increasing complexity of integrated circuit processing, the interest in relevant new materials, and the continuing success of device miniaturization, we anticipate that *in situ* TEM will have many more exciting applications in the future.

# **Acknowledgment**

I would like to thank my collaborators Ruud Tromp, Mark Reuter, Jerry Tersoff, Klaus Schwarz, Christian Lavoie, and Jim Harper, all at the IBM Thomas J. Watson Research Center, Yorktown Heights, New York, for their important contributions to the research presented here.

### References

- F. M. Ross, J. M. Gibson, and R. D. Twesten, "Dynamic Observations of Interface Motion During the Oxidation of Silicon," Surf. Sci. 310, 243–266 (1994).
- P. A. Flinn, M. C. Madden, and T. N. Marieb, "In Situ SEM Observations of Electromigration Voids in Al Lines Under Passivation," Mater. Res. Soc. Bull. 19, 51–55 (1994).
- 3. C. Weisbuch and B. Vinter, *Quantum Semiconductor Structures: Fundamentals and Applications*, Academic Press, Inc., Boston, 1991.
- R. Anderson, Ed., Specimen Preparation for Transmission Electron Microscopy of Materials II, Mater. Res. Soc. Proc. 199, Materials Research Society Press, Warrendale, PA, 1990.
- C. Hayzelden, C. J. D. Hetherington, and F. M. Ross, Eds., Electron Microscopy of Semiconducting Materials and ULSI Devices, Mater. Res. Soc. Proc. 523, Materials Research Society Press, Warrendale, PA, 1998.

<sup>&</sup>lt;sup>4</sup> Gatan Imaging Filter, Gatan, Inc., 680 Commonwealth Drive, Warrendale, PA 15086.

- M. Hammar, F. LeGoues, J. Tersoff, M. C. Reuter, and R. M. Tromp, "In Situ Ultrahigh Vacuum Transmission Electron Microscopy Studies of Heteroepitaxial Growth. I. Si(001)/Ge," Surf. Sci. 349, 129–144 (1995).
- F. M. Ross, P. A. Bennett, R. M. Tromp, J. Tersoff, and M. Reuter, "Growth of CoSi<sub>2</sub> and Ge Islands Observed with *In Situ* Transmission Electron Microscopy," *Micron* 30, 21–32 (1999).
- 8. D. J. Eaglesham and M. Cerullo, "Dislocation-Free Stranski-Krastanow Growth of Ge on Si(100)," *Phys. Rev. Lett.* **64**, 1943–1946 (1990).
- For a review see F. M. Ross, F. K. LeGoues, J. Tersoff, R. M. Tromp, and M. Reuter, "In Situ Transmission Electron Microscopy Observations of the Formation of Self-Assembled Ge Islands on Si," Microsc. Res. Tech. 42, 281–294 (1998).
- 10. D. Leonard, M. Krishnamurthy, C. M. Reaves, S. P. Denbaars, and P. M. Petroff, "Direct Formation of Quantum-Sized Dots from Uniform Coherent Islands of InGaAs on GaAs Surfaces," Appl. Phys. Lett. 63, 3203-3205 (1993); J. M. Moison, F. Houzay, F. Barthe, L. Leprince, E. Andre, and O. Vatel, "Self-Organized Growth of Regular Nanometer-Scale InAs Dots on GaAs," Appl. Phys. Lett. 64, 196-198 (1994); A. Ponchet, A. Le Corre, H. L'Haridon, B. Lambert, and S. Salaun, "Relationship Between Self-Organization and Size of InAs Islands on InP(001) Grown by Gas-Source Molecular Beam Epitaxy," Appl. Phys. Lett. 67, 1850-1852 (1995); N. P. Kobayashi, T. R. Ramachandran, P. Chen, and A. Madhukar, "In Situ Atomic Force Microscope Studies of the Evolution of InAs Three Dimensional Islands on GaAs(001)," Appl. Phys. Lett. 68, 3299-3301 (1996); C. M. Reaves, R. I. Pelzel, G. C. Hsueh, W. H. Weinberg, and S. P. Denbaars, "Formation of Self-Assembled InP Islands on a GaInP/GaAs(311)A Surface," Appl. Phys. Lett. 69, 3878-3880 (1996); S. H. Xin, P. D. Wang, A. Yin, C. Kim, M. Dobrowolska, J. L. Merz, and J. K. Furdyna, "Formation of Self-Assembling CdSe Quantum Dots on ZnSe by Molecular Beam Epitaxy," Appl. Phys. Lett. 69, 3884-3886 (1996); J. Drucker and S. Chapparro, "Diffusional Narrowing of Ge on Si(001) Coherent Island Quantum Dot Size Distributions," Appl. Phys. Lett. 71, 614-616 (1997).
- 11. M. Zinke-Allmang, L. C. Feldman, and M. H. Grabow, "Clustering on Surfaces," *Surf. Sci. Rep.* **16**, 377–463 (1992)
- V. A. Shchukin, N. N. Ledentsov, P. S. Kop'ev, and D. Bimberg, "Spontaneous Ordering of Arrays of Coherent Strained Islands," *Phys. Rev. Lett.* 75, 2968–2971 (1995);
   I. Daruka and A.-L. Barabasi, "Dislocation-Free Island Formation in Heteroepitaxial Growth: A Study at Equilibrium," *Phys. Rev. Lett.* 79, 3708–3711 (1997).
- 13. D. Leonard, K. Pond, and P. M. Petroff, "Critical Thickness for Self-Assembled InAs Islands on GaAs," *Phys. Rev. B* 50, 11687–11692 (1994); Q. Xie, N. P. Kobayashi, T. R. Ramachandran, A. Kalburge, P. Chen, and A. Madhukar, "Strained Coherent InAs Quantum Box Islands on GaAs(001): Size Equalization, Vertical Self-Organization and Optical Properties," *J. Vac. Sci. Technol. B* 14, 2203–2207 (1996); Y. Chen and J. Washburn, "Structural Transition in Large-Lattice-Mismatch Heteroepitaxy," *Phys. Rev. Lett.* 77, 4046–4049 (1996); A.-L. Barabasi, "Self-Assembled Island Formation in Heteroepitaxial Growth," *Appl. Phys. Lett.* 70, 2565–2567 (1997).
- K. M. Chen, D. E. Jesson, S. J. Pennycook, T. Thundat, and R. J. Warmack, "New Insights into the Kinetics of the Stress-Driven Two-Dimensional to Three-Dimensional Transition," J. Vac. Sci. Technol. B 14, 2199–2202 (1996).
- 15. G. Medeiros-Ribeiro, A. M. Bratkovsky, T. I. Kamins, D. A. A. Ohlberg, and R. S. Williams, "Shape Transition

- of Germanium Nanocrystals on a Silicon (001) Surface from Pyramids to Domes," Science 279, 353–355 (1998).
- 16. F. M. Ross, J. Tersoff, and R. M. Tromp, "Coarsening of Self-Assembled Ge Quantum Dots on Si(001)," *Phys. Rev. Lett.* **80**, 984–987 (1998).
- 17. R. M. Tromp and M. Mankos, "Thermal Adatoms on Si(001)," *Phys. Rev. Lett.* **81**, 1050-1053 (1998).
- T. I. Kamins and R. S. Williams, "Lithographic Positioning of Self-Assembled Ge Islands on Si(001)," *Appl. Phys. Lett.* 71, 1201–1203 (1997).
- S. Yu. Shiryaev, F. Jensen, J. Lundsgaard Hansen, J. W. Peterson, and A. Nylandsted Larsen, "Nanoscale Structuring by Misfit Dislocations in Si<sub>1-x</sub>Ge<sub>x</sub>/Si Epitaxial Systems," *Phys. Rev. Lett.* 78, 503–507 (1997); Y. H. Xie, S. B. Samavedam, M. Bulsara, T. A. Langdo, and E. A. Fitzgerald, "Relaxed Template for Fabricating Regularly Distributed Quantum Dot Arrays," *Appl. Phys. Lett.* 71, 3567–3568 (1997).
- T. Ogino, "Self Organization of Nanostructures on Si Wafers Using Surface Structure Control," Surf. Sci. 386, 137–148 (1997).
- 21. J. W. Matthews and A. E. Blakeslee, "Defects Associated with the Accommodation of Misfits Between Crystals," *J. Vac. Sci. Technol.* 12, 126–133 (1975); J. W. Matthews, A. E. Blakeslee, and S. Marder, "Use of Misfit Strain to Remove Dislocations from Epitaxial Thin Films," *Thin Solid Films* 33, 253–266 (1976); R. Hull, J. C. Bean, D. J. Werder, and R. E. Leibenguth, "In Situ Observations of Misfit Dislocation Propagation in Ge<sub>x</sub>Si<sub>1-x</sub>/Si(100)
- Heterostructures," Appl. Phys. Lett. 52, 1605 (1988).
  22. F. E. Ejeckam, Y. H. Lo, S. Subramanian, H. Q. Hou, and B. E. Hammons, "Lattice Engineered Compliant Substrate for Defect-Free Heteroepitaxial Growth," Appl. Phys. Lett. 70, 1685–1687 (1997).
- J. Lasky, J. Nakos, O. Cain, and P. Geiss, "Comparison of Transformation to Low-Resistivity Phase and Agglomeration of TiSi, and CoSi<sub>2</sub>," *IEEE Trans. Electron Devices* 38, 262 (1991).
- 24. S. P. Murarka, D. B. Fraser, M. Eizenberg, R. Tung, and R. Madar, Eds., Advanced Interconnects and Contact Materials and Processes for Future Integrated Circuits, Mater. Res. Soc. Proc. 514, Materials Research Society Press, Warrendale, PA, 1998.
- C. Cabral, Jr., L. A. Clevenger, J. M. E. Harper, F. M. d'Heurle, R. A. Roy, C. Lavoie, K. L. Saenger, G. L. Miles, R. W. Mann, and J. S. Nakos, "Low Temperature Formation of C54-TiSi<sub>2</sub> Using Titanium Alloys," *Appl. Phys. Lett.* 71, 3531–3533 (1997).

Received July 12, 1999; accepted for publication October 15, 1999

Frances M. Ross IBM Research Division, Thomas J. Watson Research Center, P.O. Box 218, Yorktown Heights, New York 10598 (fmross@us.ibm.com). Dr. Ross is a Research Staff Member in the Physical Sciences Department at the Thomas J. Watson Research Center. She received her B.A. degree in physics and her Ph.D. degree in materials science from Cambridge University in 1985 and 1989, respectively. She then joined A.T.&T. Bell Laboratories in 1990 as a Postdoctoral Member of Technical Staff, where she made use of in situ electron microscopy techniques to study silicon oxidation and the formation of dislocations in SiGe alloys. From 1992 to 1997 she worked as a Staff Scientist at the National Center for Electron Microscopy, Lawrence Berkeley National Laboratory, where she used in situ microscopy to observe the anodic etching of silicon and the motion of domain walls in ferroelectrics, as well as coordinating users of the High Resolution and In Situ facilities. In 1997 she joined IBM as a Research Staff Member. Dr. Ross is currently studying growth processes in semiconductors and silicides and is also developing a novel specimen geometry for the study of reactions at liquid/solid interfaces. In 1999 she received the Institute of Physics Charles Vernon Boys Medal for her contributions to real-time visualization of materials growth and processing. She is an author or co-author of thirty journal articles and one patent.